AtRMR1 functions as a cargo receptor for protein trafficking to the protein storage vacuole

Misoon Park, Daeseok Lee, Gil-Je Lee, and Inhwan Hwang

Division of Molecular and Life Sciences, Center for Plant Intracellular Trafficking, Pohang University of Science and Technology, Pohang 790-784, Korea

Organellar proteins are sorted by cargo receptors on the way to their final destination. However, receptors for proteins that are destined for the protein storage vacuole (PSV) are largely unknown. In this study, we investigated the biological role that *Arabidopsis thaliana* receptor homology region transmembrane domain ring H2 motif protein (AtRMR) 1 plays in protein trafficking to the PSV. AtRMR1 mainly colocalized to the prevacuolar compartment of the PSV, but a minor portion also localized to the Golgi complex. The coexpression of AtRMR1 mutants that were localized to the Golgi complex strongly inhibited the trafficking of phaseolin to the PSV and caused accumulation of phaseolin in the Golgi complex or its secretion. Coimmunoprecipitation and in vitro binding assays revealed that the lumenal domain of AtRMR1 interacts with the COOH-terminal sorting signal of phaseolin at acidic pH. Furthermore, phaseolin colocalized with AtRMR1 on its way to the PSV. Based on these results, we propose that AtRMR1 functions as the sorting receptor of phaseolin for its trafficking to the PSV.

Introduction

The protein storage vacuole (PSV) was originally identified as an intracellular organelle that stores proteins in seed cells (Müntz, 1998). However, it was recently found that the PSV or an equivalent organelle is also present in many different types of plant cells, including leaf and root cells (Jiang and Rogers, 1998; Jiang et al., 2000; Park et al., 2004). Leaf and root cells also contain the large central vacuole that functions as the lytic vacuole. Thus, certain types of plant cells contain multiple species of vacuoles.

The presence of these multiple vacuoles (the PSV and the lytic vacuole in plant cells) poses interesting questions regarding the trafficking of proteins to these compartments (Müntz, 1998; Jiang and Rogers, 1998; Jiang et al., 2000; Park et al., 2004). Proteins that are destined for the lytic vacuole are transported from the ER through the Golgi complex and prevacuolar compartment (PVC). This trafficking pathway appears to be quite similar to the pathway that directs proteins to the lysosome and the vacuole in animal and yeast cells, respectively (for review see Vitale and Raikhel, 1999; Bassham and Raikhel, 2000; Jin et al., 2001; Kim et al., 2001; Paris and Neuhaus, 2002; Sohn et al., 2003). In contrast, the mechanisms by which proteins are trafficked to the PSV may only occur in plant cells (Galili et al., 1993; Müntz, 1998; Vitale and Raikhel 1999; Park et al., 2004). Depending on the cargo protein in question, proteins are transported from the ER to the PSV through multiple pathways (Hara-Nishimura et al., 1998; Toyooka et al., 2000; Park et al., 2004). Many storage proteins, such as 7S and 11S class proteins, and defense proteins like lectins are transported through the Golgi complex and are transported to the PSV by dense vesicles (DVs; Chrispeels, 1983; Herman and Shannon, 1984; Greenwood and Chrispeels, 1985; Hohl et al., 1996; Hinz et al., 1999; Hillmer et al., 2001; Kinney et al., 2001). In this pathway, proteins are sorted mainly at the cis half of the Golgi stack into developing DVs, and mature DVs are released from the TGN to deliver storage proteins to the PSV (Hillmer et al., 2001). In contrast, storage globulins in pumpkin seeds and a cysteine proteinase containing a transient ER retention signal may be transported to PSVs in a Golgi-independent manner by large vesicles that are termed precursor-accumulating (PAC) or KDEL (Lys-Asp-Glu-Leu) vesicles (Hara-Nishimura et al., 1998; Toyooka et al., 2000). Wheat storage proteins are also, in part, delivered to the PSV via a Golgi-independent route (Galili et al., 1993). Another class of protein that is transported to the PSV through the

Correspondence to Inhwan Hwang: ihhwang@postech.ac.kr

Abbreviations used in this paper: AALP, *Arabidopsis* aleurain-like protease; AtRMR, *Arabidopsis thaliana* RMR; BiP, binding protein; COP, coat protein complex; CT, cytosolic tail; CTPP, COOH-terminal propeptide; DIP, dark-induced tonoplastic intrinsic protein; DV, dense vesicle; LU, lumenal domain; MBP, maltose-binding protein; NTPP, NH_2-terminal propeptide; PAC, precursor accumulating; PSV, protein storage vacuole; PVC, prevacuolar compartment; RMR, receptor homology region transmembrane domain ring H2 motif protein; ST, sialyltransferase; TIP, tonoplast intrinsic protein; VSR, vacuolar sorting receptor.

The online version of this article contains supplemental material.

The Journal of Cell Biology, Vol. 170, No. 5, August 29, 2005 757–767
http://www.jcb.org/cgi/doi/10.1083/jcb.200504112

Golgi-independent pathway is α-tonoplast intrinsic protein (TIP), which is a membrane protein that localizes to the PSV (Gomez and Chrispeels, 1993; Jiang and Rogers, 1998; Park et al., 2004).

Three different types of signal sequences on proteins that are targeted to vacuoles through the Golgi complex have been identified. These include the COOH-terminal propeptide (CTPP), the NH_2-terminal propeptide (NTPP), and the internal targeting determinant (Matsuoka et al., 1990; Bednarek and Raikhel, 1991; Neuhaus et al., 1991; Chrispeels and Raikhel, 1992; Saalbach et al., 1996; Frigerio et al., 1998). In addition, it is believed that transient aggregation may aid the targeting of protein to the PSV via the Golgi-independent pathway (Holkeri and Vitale, 2001).

The molecular players that are involved in these various PSV-trafficking pathways are largely unknown. In particular, there is very limited information on the proteins that participate in the PSV-trafficking pathways. One of these may be BP-80/vacuolar sorting receptor (VSR) homologues. In pea cotyledon, BP-80 localizes to the TGN (Hillmer et al., 2001). In *Arabidopsis thaliana*, AtVSR1 has been shown to localize to the TGN or PVC (Kirsch et al., 1994; Ahmed et al., 2000; Paris and Neuhaus, 2002). Recently, it has been suggested that AtVSR1, the *A. thaliana* homologue of BP-80, functions as the receptor for PSV-destined proteins in seed cells (Shimada et al., 2003), although it was originally thought to be a receptor for lytic vacuolar proteins (Jiang and Rogers, 1998; Neuhaus and Rogers, 1998; Ahmed et al., 2000; Cao et al., 2000). Another molecule is PV72, which localized to the PAC vesicle and mediates the direct transport from the ER to PSV (Shimada et al., 2002). In addition, receptor homology region transmembrane domain ring H2 motif protein (RMR) has been proposed to act as a possible receptor for PSV-destined proteins (Jiang et al., 2000).

In this study, we investigated the possibility that *A. thaliana* RMR (AtRMR) 1 may function as a receptor for PSV-destined proteins by using phaseolin as a model cargo protein. We demonstrate that AtRMR1 mainly colocalizes with dark-induced tonoplastic intrinsic protein (DIP) to the PVC of the PSV in *A. thaliana* leaf protoplasts and interacts with the CTPP of phaseolin in a pH-dependent manner. Furthermore, coexpression of AtRMR1 deletion mutants strongly inhibits the trafficking of phaseolin to the PSV and causes secretion of phaseolin into the medium.

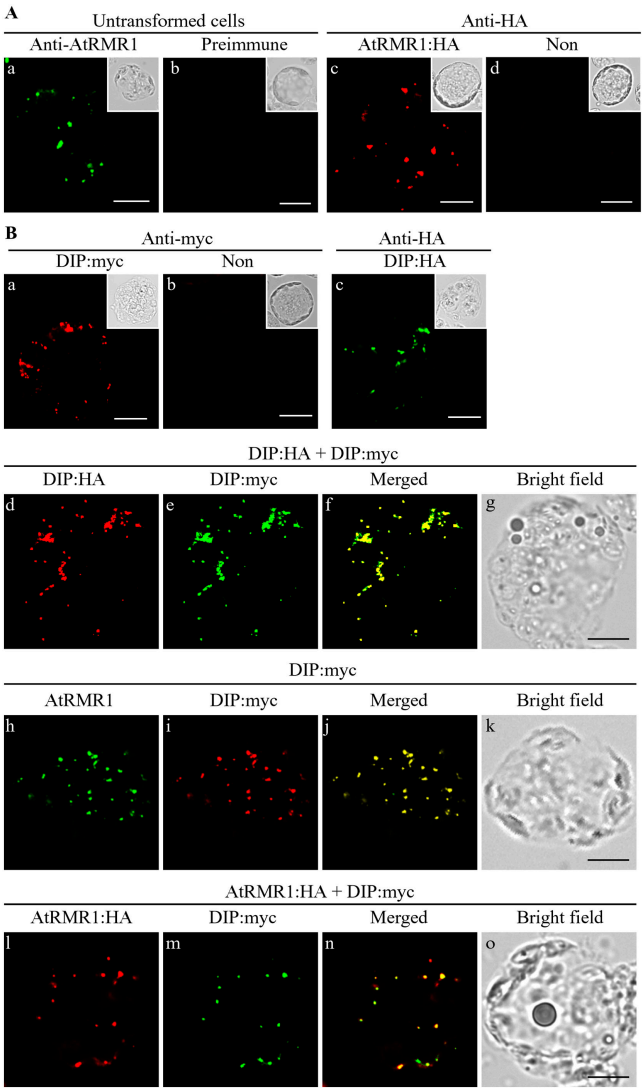

Figure 1. **AtRMR1 localizes primarily to the DIP-positive organelle.** (A) Localization of AtRMR1 and AtRMR1-HA. Untransformed (Non) or *AtRMR1-HA*–transformed (AtRMR1-HA) protoplasts were fixed and stained with anti-AtRMR1 or anti-HA antibodies, respectively. As a control, preimmune serum was used to stain untransformed protoplasts. Insets, bright field images. (B) Colocalization of AtRMR1 and AtRMR1-HA with DIP-myc. Protoplasts transformed with the indicated constructs were stained with anti-myc, anti-HA, or anti-AtRMR1 antibodies. AtRMR1, endogenous AtRMR1 detected with anti-AtRMR1 antibody; Non, untransformed protoplasts. Bars, 20 μm.

Results

AtRMR1 localizes to the DIP-positive organelle in *A. thaliana* leaf protoplasts

It has been shown previously that the *A. thaliana* genome encodes multiple isoforms of RMR (Jiang et al., 2000; Fig. S1, available at http://www.jcb.org/cgi/content/full/jcb.200504112/DC1). When detected with anti-RMR antibodies raised against an *AtRMR* isoform (the RMR isoform encoded by the cDNA clone JR702; Jiang et al., 2000), RMR yields a punctate staining pattern and colocalizes with DIP, which is an isoform of TIP (Jiang et al., 2000), in root tip cells and mature seed cells. The punctate stains of these proteins were located within the PSV that was marked by δ- and α-TIP. To investigate the biological role played by AtRMR1 (Fig. S1), we examined its expression and localization in leaf cells. RT-PCR analysis using *AtRMR1*-specific primers revealed that *AtRMR1* is expressed in most *A. thaliana* tissues regardless of the growth stage of the plant (Fig. S2, available at http://www.jcb.org/cgi/content/full/jcb.200504112/DC1). To examine the localization of AtRMR1 in leaf cells, we generated an antibody against the COOH-terminal domain of AtRMR1 (Fig. S3, available at http://www.jcb.org/cgi/content/full/jcb.200504112/DC1). In addition, we generated HA epitope–tagged AtRMR1 (AtRMR1-HA; Fig. S3). We examined AtRMR1 localization in leaf cells by immunohistochemistry using anti-AtRMR1 and anti-HA an-

tibodies. We prepared two different samples—untransformed and *AtRMR1-HA*–transformed protoplasts—and stained them with anti-AtRMR1 and anti-HA antibodies, respectively (Frigerio et al., 2001; Sohn et al., 2003). Both anti-AtRMR1 and anti-HA antibodies gave punctate staining patterns in untransformed and *AtRMR1-HA*–transformed protoplasts, respectively (Fig. 1 A). As a control, we stained untransformed protoplasts with control preimmune serum and anti-HA antibody but did not observe any punctate stains (Fig. 1 A, b and d). To identify AtRMR1-positive organelles, we examined whether AtRMR1 colocalizes with DIP. DIP, a homologue of tonoplastic water channel, is expressed in root tip cells and seed cells from tobacco and gives punctate staining patterns. In mature seed and root tip cells, these punctate stains were detected within the PSV. In contrast, in immature seed cells, these punctate stains were observed outside the PSV. However, the function of DIP has not been clearly defined yet. We expressed myc- or HA-tagged tobacco DIP (DIP-myc and DIP-HA) in leaf cell protoplasts (Fig. S4, available at http://www.jcb.org/cgi/content/full/jcb.200504112/DC1). Both anti-myc and anti-HA antibodies gave the same punctate staining pattern in the transformed protoplasts (Fig. 1 B, a and c). Furthermore, punctate stains that were observed with the anti-myc antibody closely overlapped with those detected with the anti-HA antibody (Fig. 1 B, d–g). Next, we examined colocalization of AtRMR1 and AtRMR1-HA with DIP-myc in protoplasts. A majority of endogenous AtRMR1-positive punctate stains that were detected with anti-AtRMR1 antibody colocalized with the DIP-myc stains (Fig. 1 B, h–k). In addition, a majority of punctate stains of transiently expressed AtRMR1-HA colocalized with those of DIP-myc (Fig. 1 B, l–o). These results indicate that a majority of both endogenous and transiently expressed AtRMR1 colocalizes with DIP-myc in protoplasts. Furthermore, these results imply that transiently expressed AtRMR1-HA behaves in the same way as endogenous AtRMR1.

To further define the organelle to which AtRMR1 localizes, we compared its localization with that of other organellar marker proteins. When protoplasts were cotransformed with *AtRMR1-HA* and *sialyltransferase* (*ST*)*-GFP,* which is a marker of the Golgi complex (Lee et al., 2002), both proteins gave punctate staining patterns. As expected, the majority of AtRMR1-HA did not colocalize with ST-GFP. However, a small fraction of the punctate stains consisted of overlapping AtRMR1-HA and ST-GFP signals (Fig. 2, c–f). To confirm this, we examined the colocalization of AtRMR1-HA with endogenous γ–coat protein complex (COP), which is a component of the COPI vesicle that localizes to the Golgi complex (Fig. 2, g–j; Pimpl et al., 2000). Again, a minor portion of AtRMR1-HA–positive punctate stains overlapped with γ-COP stains. To estimate the relative distribution of AtRMR1-HA between these two different organelles, we counted the punctate stains of AtRMR1-HA that overlapped with those of DIP-myc, ST-GFP, or γ-COP. AtRMR1-HA stains overlapped with these proteins 77, 23, and 24% of the time, respectively (Fig. S5, available at http://www.jcb.org/cgi/content/full/jcb.200504112/DC1). This shows that AtRMR1-HA in *A. thaliana* leaf protoplasts mainly localizes to the DIP-positive organelle but is also found, at lower levels, in the Golgi complex.

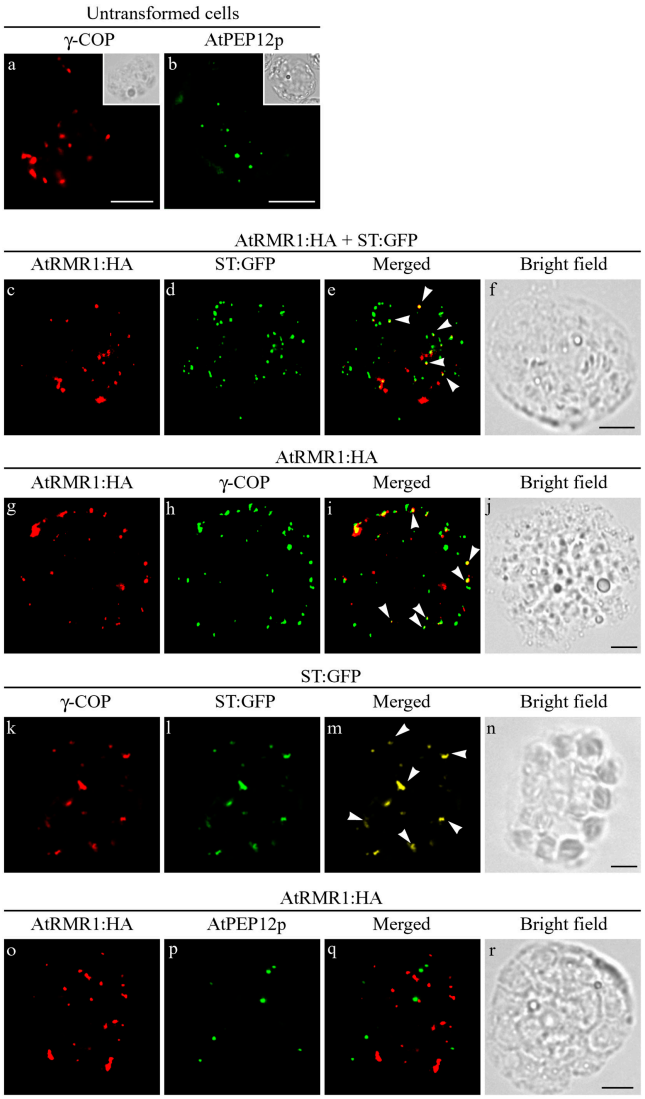

Figure 2. **A minor portion of AtRMR1 localizes to the Golgi complex.** Protoplasts were transformed with the indicated constructs. ST-GFP was directly observed with green fluorescent signals from the fixed protoplasts. AtRMR1-HA was detected with anti-HA antibody. Endogenous γ-COP and AtPEP12p were detected with anti–γ-COP and anti-AtPEP12p antibodies, respectively. (a and b) Insets show bright field images. Arrowheads indicate overlaps between the indicated proteins. Bars, 20 μm.

Next, we transformed protoplasts with *AtRMR1-HA* and examined the colocalization of AtRMR1-HA with endogenous AtPEP12p, which is a marker for the PVC of the lytic vacuole (da Silva Conceicao et al., 1997), by immunohistochemistry using anti-HA and anti-AtPEP12p antibodies (Fig. 2, o–r). Both AtRMR1-HA and endogenous AtPEP12p gave punctate staining patterns, but no colocalization was observed, which indicates that AtRMR1-HA does not localize at the PVC of the lytic vacuole.

Coexpression of AtRMR1 deletion mutants inhibits the trafficking of phaseolin to the PSV

A previous study suggested that RMR may play a role in protein trafficking to the PSV (Jiang et al., 2000). To investigate

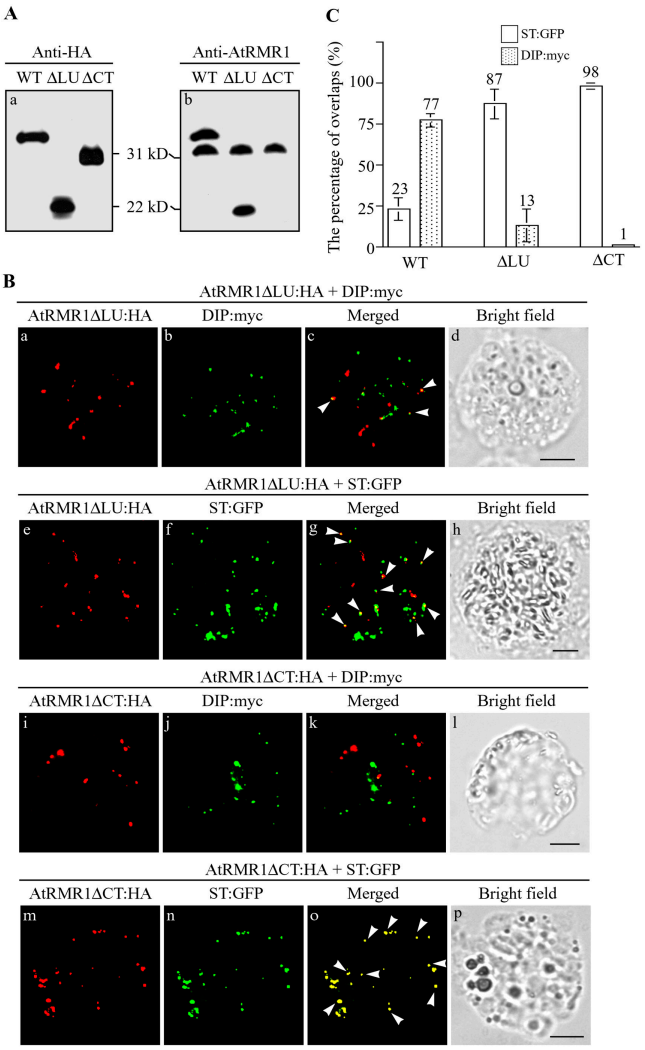

Figure 3. **Localization of AtRMR1 deletion mutants.** (A) Expression of AtRMR1 deletion mutants. Protein extracts were obtained from protoplasts transformed with the indicated constructs and subjected to Western blot analysis using anti-HA and anti-AtRMR1 antibodies. Note that anti-AtRMR1 antibody does not recognize AtRMR1ΔCT. (B) Localization of AtRMR1 deletion mutants. Protoplasts transformed with the indicated constructs were fixed and stained with anti-HA or anti-myc antibodies. The green fluorescent signal of ST-GFP was directly observed from fixed protoplasts. Arrowheads indicate overlaps between the indicated proteins. Bars, 20 μm. (C) Quantification of the overlaps between AtRMR1 deletion mutants and ST-GFP or DIP-myc. The number of punctate stains of AtRMR1 deletion mutants and ST-GFP or DIP-myc that overlapped were counted to determine localization of AtRMR1 deletion mutants. More than 200 punctate stains of AtRMR1 deletion mutants were counted for each comparison in a triplicate experiment. Error bars represent SEM. WT, wild-type AtRMR1; ΔLU, AtRMR1ΔLU-HA; ΔCT, AtRMR1ΔCT-HA.

this possibility, we examined whether AtRMR1 deletion mutants could inhibit protein trafficking to the PSV through a dominant negative effect. AtRMR1 consists of various domains: the signal peptide (aa 1–27), the lumenal domain (LU; aa 47–149), the transmembrane region (aa 170–190), and the cytosolic ring H2 finger domain (cytosolic tail [CT], aa 222–273; Fig. S6, available at http://www.jcb.org/cgi/content/full/jcb.200504112/DC1). LU may interact with cargo molecules, whereas CT may interact with a cytoplasmic component that is involved in trafficking. We transformed *A. thaliana* leaf protoplasts with two HA-tagged *AtRMR1* deletion mutant constructs, *AtRMR1ΔLU-HA* and *AtRMR1ΔCT-HA,* as well as with the corresponding wild-type construct (Fig. S6) and examined their expression by Western blot analysis using anti-HA antibody. AtRMR1ΔLU-HA and AtRMR1ΔCT-HA were detected at the positions of 22 and 30 kD (Fig. 3 A, a), respectively. The expression levels of these transiently expressed wild-type and deletion mutants of AtRMR1-HA were nearly the same as those of endogenous AtRMR1 (Fig. 3 A, b). The polyethylene glycol–mediated transformation efficiency of protoplasts was 30–50% (not depicted; Jin et al., 2001). Thus, the level of transiently expressed AtRMR1 is two- to threefold higher than that of endogenous AtRMR1 in transformed protoplasts. Protoplasts were then transformed with these mutants together with *DIP-myc* or *ST-GFP* and were immunostained using anti-HA and anti-myc antibodies. Like wild-type AtRMR1-HA, AtRMR1ΔLU-HA gave a punctate staining pattern, but the majority (87%) of the punctate stains of AtRMR1ΔLU-HA overlapped those of ST-GFP (Fig. 3, B [e–h] and C), and only a minor portion (13%) of AtRMR1ΔLU-HA–positive punctate stains were colocalized with those of DIP-myc (Fig. 3, B [a–d] and C). Furthermore, nearly all of the AtRMR1ΔCT-HA–positive punctate stains colocalized with ST-GFP (Fig. 3, B [m–p] and C). These results suggest that both LU and the cytoplasmic ring H2 region are important for the localization of AtRMR1-HA to the DIP-positive organelle.

Next, we examined the effect of these AtRMR1 deletion mutants on the trafficking of phaseolin, which is a storage protein of the common bean (Frigerio et al., 1998). Phaseolin has been shown to be targeted to the PSV when it is transiently expressed in leaf protoplasts (Park et al., 2004). In *A. thaliana* leaf protoplasts that express phaseolin, ∼70% of protoplasts show the disc pattern that indicates targeting to the PSV, whereas the remaining 30% of protoplasts show network or punctate staining patterns (Park et al., 2004). Protoplasts were cotransformed with phaseolin together with *AtRMR1-HA*, *AtRMR1ΔLU-HA*, or *AtRMR1ΔCT-HA*, and the localization of phaseolin was examined by immunostaining with antiphaseolin antibody. In the presence of AtRMR1-HA, the majority of protoplasts gave the typical disc pattern, as observed when phaseolin alone is expressed, which indicates that phaseolin continues to be targeted to the PSV in the presence of AtRMR1-HA (Fig. 4 A, a). However, in the presence of both AtRMR1ΔLU-HA and AtRMR1ΔCT-HA, the majority of transformed protoplasts produced a punctate staining pattern (Fig. 4 A, b and c). This indicates that the normal trafficking of phaseolin to the PSV is perturbed by the coexpression of AtRMR1 deletion mutants. To estimate the trafficking efficiency of phaseolin to the PSV, we counted protoplasts bearing the disc pattern. The presence of AtRMR1ΔLU-HA and AtRMR1ΔCT-HA reduced the phaseolin trafficking efficiency to 27 and 45%, respectively, from 70% in the presence of AtRMR1-HA (Fig. 4 B). Thus, AtRMR1 deletion mutants inhibit the trafficking of phaseolin to the PSV.

To determine the specificity of AtRMR1, we examined the effect of AtRMR1 deletion mutants on protein trafficking to the lytic vacuole. Sporamin-GFP and *Arabidopsis* aleurain-like pro-

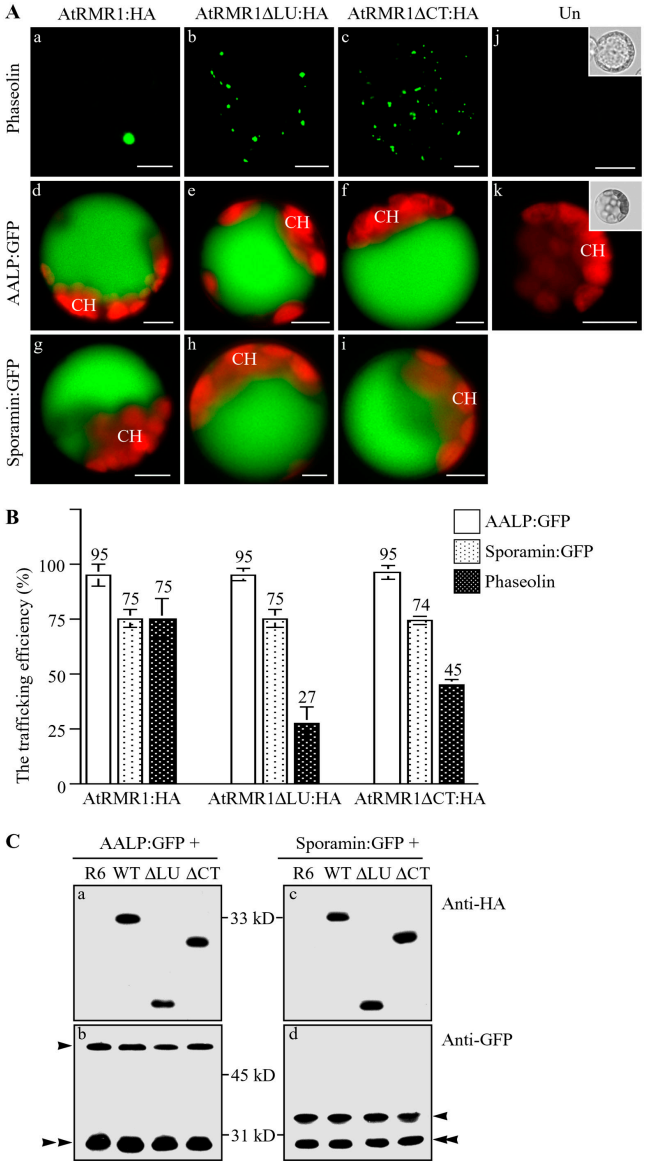

Figure 4. **AtRMR1 deletion mutants inhibit the trafficking of phaseolin to the PSV.** (A) Inhibition of phaseolin trafficking to the PSV by AtRMR1 deletion mutants. Protoplasts were transformed with the indicated constructs, and localization of the reporter proteins was examined. GFP signals of AALP-GFP and sporamin-GFP were observed from intact protoplasts, whereas phaseolin was detected from fixed protoplasts by immunostaining with antiphaseolin antibody. Un, untransformed protoplasts; CH, chloroplasts. Insets, bright field images of protoplasts. Bars, 20 μm. (B) Quantification of trafficking efficiency. To estimate the trafficking efficiency, transformed protoplasts were counted based on their GFP or immunostaining patterns. More than 100 protoplasts were counted for each transformation in a triplicate experiment. The numbers and error bars indicate the means and SEM, respectively. (C) Western blot analysis of vacuolar trafficking of AALP-GFP and sporamin-GFP. Protein extracts were prepared from protoplasts transformed with the indicated constructs and used for Western blot analysis using anti-HA or anti-GFP antibodies. WT, wild-type AtRMR1; ΔLU, AtRMR1ΔLU-HA; ΔCT, AtRMR1ΔCT-HA; R6, an empty vector used to balance the amount of plasmid DNA that was introduced into protoplasts. Single arrowhead, precursor; double arrowhead, proteolytically processed form.

tease (AALP)–GFP are targeted to the lytic vacuole through the Golgi complex in *A. thaliana* (Kim et al., 2001; Sohn et al., 2003). In the presence or absence of AtRMR1ΔLU-HA and AtRMR1ΔCT-HA, the majority of protoplasts gave green fluorescent signals in the lytic vacuole (Fig. 4 A, d–i). To estimate trafficking efficiency to the lytic vacuole, we counted the number of protoplasts with green fluorescent signals in the lytic vacuole. The trafficking efficiency of AALP-GFP and sporamin-GFP to the lytic vacuole was independent of the nature of the transforming AtRMR1 protein (Fig. 4 B), indicating that deletion mutants did not affect trafficking of these proteins to the lytic vacuole. To further confirm this observation at the protein level, protein extracts were prepared from the transformed protoplasts, and the amount of processed reporter protein was determined by Western blot analysis using anti-GFP antibody. AALP-GFP and sporamin-GFP are detected as smaller 30-kD forms when they are targeted to the vacuole as a result of proteolytic processing (Sohn et al., 2003). The amount of processed AALP-GFP and sporamin-GFP in the presence of AtRMR1 deletion mutants was nearly the same as that in the presence of wild type or the control vector R6 (Fig. 4 C). Thus, AtRMR1 deletion mutants do not affect the trafficking of proteins to the lytic vacuole.

Next, to understand how AtRMR1 deletion mutants inhibit trafficking to the PSV, we examined the identity of the organelle in which phaseolin accumulated in the presence of AtRMR1 deletion mutants. One possibility is that phaseolin may accumulate in the Golgi complex because these deletion mutants mainly localize there. Thus, protoplasts were cotransformed with *phaseolin*, *AtRMR1ΔLU-HA*, and *ST-GFP* or *phaseolin*, *AtRMR1ΔCT-HA*, and *ST-GFP*, and the localization of these proteins was examined. In both cases, the punctate stains of phaseolin that were detected with antiphaseolin antibody closely overlapped with the green fluorescent signal of ST-GFP at the Golgi complex (Fig. 5 A, e–l), which suggests that defective AtRMR1 mutants fail to deliver phaseolin to the PSV. Thus, phaseolin accumulates in the Golgi complex in the presence of AtRMR1 deletion mutants. To confirm this notion at the biochemical level, we examined the glycosylation pattern of phaseolin in the presence of deletion mutants. Phaseolin was resistant to endoH digestion in the presence of deletion mutants, which was similar to the presence of AtRMR1-HA (Fig. 5 B). In addition, a portion of phaseolin was subjected to proteolytic processing even in the presence of coexpressed AtRMR1ΔLU or AtRMR1ΔCT. This indicates that phaseolin is transported to the Golgi or post-Golgi compartments even in the presence of deletion mutants. Next, we examined the glycosylation pattern of AtRMR1 proteins. As expected from localization (Fig. 3 B), AtRMR1ΔCT-HA was also resistant to endoH (Fig. 5 B). As a control for endoH treatment, phaseolin was obtained from protoplasts coexpressing AtSar1[H74L], which is known to inhibit COPII-dependent anterograde trafficking (Takeuchi et al., 2000), and it was examined for sensitivity to endoH. It was found to be sensitive to endoH, as indicated by its faster migration in SDS gel (Fig. 5 B, asterisks). These results are consistent with the notion that phaseolin localizes at the Golgi complex in the presence of AtRMR1 deletion mutants.

Next, we examined the possibility that phaseolin is secreted into the medium in the presence of AtRMR1 deletion mutants. PhaseolinΔ418, which lacks the COOH-terminal targeting signal, is known to be secreted into the medium (Frigerio et al.,

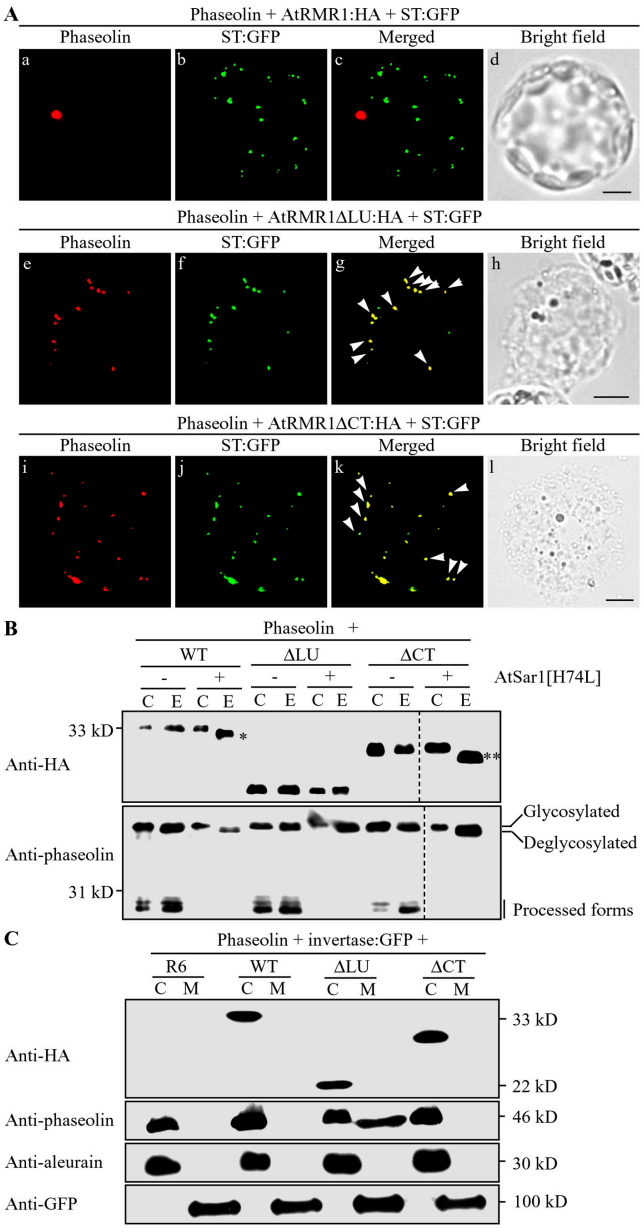

Figure 5. **Phaseolin accumulates in the Golgi complex in the presence of deletion mutants.** (A) Localization of phaseolin in the presence of deletion mutants. Protoplasts were transformed with the indicated constructs, and localization of phaseolin was examined. Phaseolin was detected from the fixed protoplasts with antiphaseolin antibody, whereas the GFP signals of ST-GFP were directly observed. Arrowheads indicate overlaps between the indicated proteins. Bars, 20 μm. (B) EndoH resistance of the glycan moiety of phaseolin in the presence of AtRMR1 deletion mutants. Protein extracts were obtained from protoplasts transformed with the indicated constructs, treated with endoH, and analyzed by Western blotting using antiphaseolin and anti-HA antibodies that detect phaseolin and HA-tagged AtRMR1 deletion mutants, respectively. Single and double asterisks indicate deglycosylated forms of AtRMR1-HA and AtRMR1ΔCT-HA, respectively. C, control protein extracts; E, endoH-treated protein extracts. Dotted lines indicate that two separate images were brought together to generate a single composite image. (C) Secretion of phaseolin in the presence of coexpressed AtRMR1ΔLU-HA. Phaseolin and invertase-GFP were coexpressed in protoplasts together with the indicated *AtRMR1* constructs. Proteins secreted from the protoplasts were prepared from the incubation medium (M). In addition, protein extracts were prepared from the transformed protoplasts (C). Phaseolin, endogenous aleurain, and invertase-GFP were detected using antiphaseolin, antialeurain, and anti-GFP antibodies, respectively. HA-tagged AtRMR1 deletion mutants were detected with anti-HA antibody. R6, an empty vector; WT, wild-type AtRMR1; ΔLU, AtRMR1ΔLU-HA; ΔCT, AtRMR1ΔCT-HA.

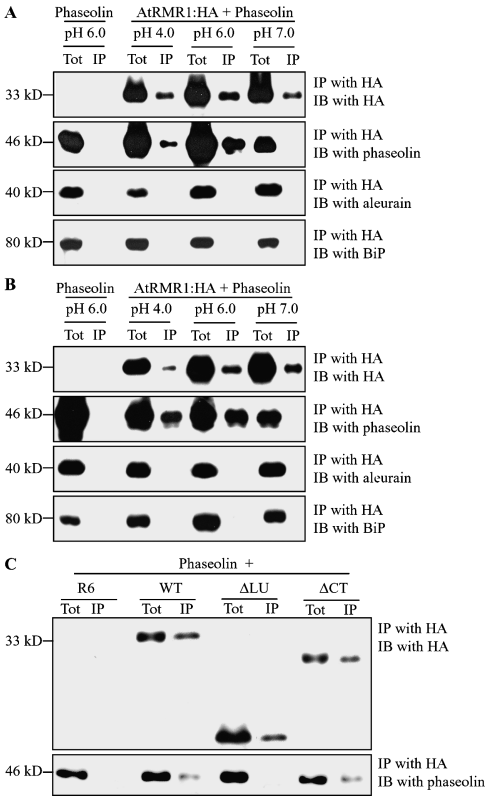

Figure 6. **AtRMR1-HA interacts with phaseolin.** (A and B) Coimmunoprecipitation of phaseolin with AtRMR1-HA in the presence of 1 mM Ca^{2+} (A) or 10 mM EDTA (B). Protein extracts were obtained from protoplasts transformed with *phaseolin* alone or together with *AtRMR1-HA* and used for immunoprecipitation using anti-HA antibody. Immunoprecipitation was performed at different pH conditions in the presence of 1 mM Ca^{2+} or 10 mM EDTA. The pellet fractions were then subjected to immunoblot analysis (IB) with anti-HA, antiphaseolin, anti-BiP, or antialeurain antibodies (note that aleurain is the precursor form). (C) Immunoprecipitation of phaseolin with deletion mutants. Phaseolin was expressed in protoplasts together with the indicated *AtRMR1* constructs. Protein extracts were prepared from the transformed protoplasts and used for coimmunoprecipitation using anti-HA antibody. The pellet fractions were then subjected to immunoblot analysis (IB) using anti-HA and antiphaseolin antibodies. Tot, total protein extracts; IP, immunoprecipitated fraction; R6, an empty vector; WT, wild-type AtRMR1; ΔLU, AtRMR1ΔLU-HA; ΔCT, AtRMR1ΔCT-HA.

1998). Proteins in the protoplast incubation medium and proteins extracted from transformed protoplasts (Park et al., 2004) were prepared separately for Western blot analysis. AtRMR1ΔLU-HA but not wild type or AtRMR1ΔCT-HA caused the secretion of ~60% of phaseolin into the medium (Fig. 5 C). As controls, we examined whether AtRMR1ΔLU-HA causes secretion of other vacuolar proteins. The vacuolar protein aleurain (Ahmed et al., 2000) was not secreted into the medium in the presence of coexpressed AtRMR1 deletion mutants. Additionally, the secretion of invertase-GFP, a fusion protein between secretory invertase and GFP (Sohn et al., 2003), was unaffected by any of the mutant or wild-type HA constructs.

AtRMR1-HA interacts with phaseolin in vivo

To obtain more direct evidence that AtRMR1 plays a role in the trafficking of phaseolin to the PSV, we examined whether

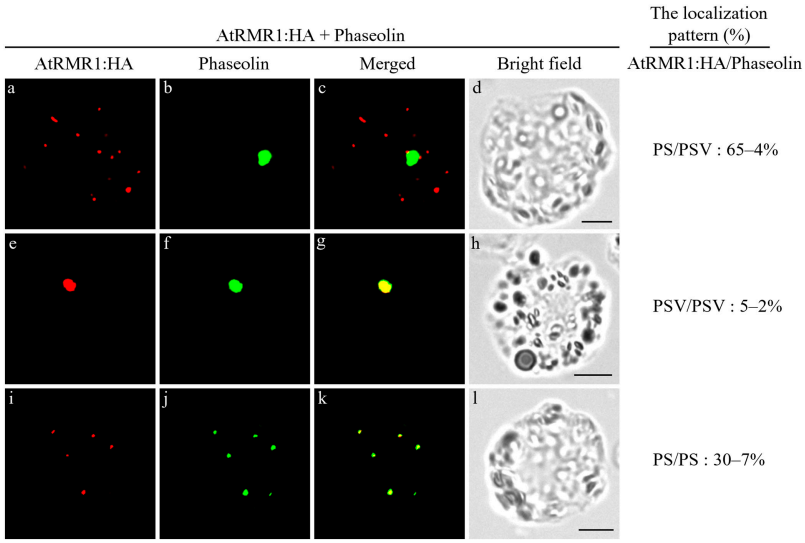

Figure 7. **Colocalization of phaseolin with AtRMR1-HA.** Protoplasts were transformed with *phaseolin* together with *AtRMR1-HA*, and localization of both of these proteins was examined by immunostaining with antiphaseolin and anti-HA antibodies. To quantify the localization patterns of AtRMR1-HA and phaseolin, the protoplasts were counted based on their immunostaining pattern. More than 100 protoplasts were counted for each protein. Three independent experiments were performed to obtain means and SEM. PS, small punctate staining pattern; PSV, disc pattern. Bars, 20 μm.

AtRMR1 interacts with phaseolin in the cell. To do this, we used a coimmunoprecipitation approach. Coimmunoprecipitation was performed in various pH conditions. It is well known that compartments in the endomembrane system are acidic (Taiz, 1992; Sun-Wada et al., 2003), whereas the PSV has neutral or near neutral pH (Swanson et al., 1998). In addition, we examined the effect of Ca^{2+} on the interaction because, in cases of vacuolar sorting receptors PV72 and AtVSR1, Ca^{2+} is critical for interaction with their cargo 2S proalbumin (Shimada et al., 2002; 2003). *A. thaliana* protoplasts were transformed with *phaseolin* with or without *AtRMR1-HA*, and protein extracts were prepared. AtRMR1-HA was first immunoprecipitated with anti-HA antibody in the presence of 1 mM Ca^{2+} at various pH conditions. The pellet fraction was then probed with anti-HA, antiphaseolin, antialeurain, and antibinding protein (BiP) antibodies. Antialeurain and anti-BiP antibodies (Jiang and Rogers, 1998; Lee et al., 2002) were used as controls for nonspecific interactions. AtRMR1-HA was detected in the pellet fractions that were obtained with anti-HA antibody at various pH conditions (Fig. 6 A). Phaseolin was detected in the anti-HA antibody immunoprecipitates that were obtained at pH 4.0 and 6.0 but not in the precipitates that were obtained at pH 7.0. Thus, AtRMR1-HA interacts with phaseolin in protoplasts in acidic conditions. At these conditions, BiP that was present in the ER was not precipitated together with AtRMR1-HA. Furthermore, AtRMR1-HA was not coimmunoprecipitated with aleurain, which is a vacuolar protein that is known to traffic through the Golgi complex to the vacuole (Ahmed et al., 2000). This observation is consistent with results showing that AtRMR1 deletion mutants do not inhibit trafficking of AALP-GFP to the lytic vacuole. Altogether, the results suggest that the interaction between AtRMR1-HA and phaseolin is specific. Next, we performed coimmunoprecipitation experiments in the presence of 10 mM EDTA. The presence of EDTA did not alter the acid-dependent association of phaseolin with AtRMR1-HA (Fig. 6 B). Thus, AtRMR1-HA interacts with phaseolin in vivo in a Ca^{2+}-independent manner. In addition, phaseolin was coimmunoprecipitated with AtRMR1ΔCT-HA but not with AtRMR1ΔLU-HA by anti-HA antibody, which indicates that the LU of AtRMR1 mediates the interaction between AtRMR1 and phaseolin (Fig. 6 C).

To confirm the interaction between AtRMR1-HA and phaseolin, we examined whether and where these two proteins colocalize with each other. To address these questions, protoplasts were cotransformed with *AtRMR1-HA* and *phaseolin*, and the localization of both of these proteins was examined by immunostaining using anti-HA and antiphaseolin antibodies, respectively. When *A. thaliana* leaf protoplasts are transformed with phaseolin alone, ~70% show a disc pattern that indicates targeting to the PSV, whereas the remaining protoplasts show either network or small punctate staining patterns (Park et al., 2004). When phaseolin and AtRMR1-HA were coexpressed, we found that phaseolin was again distributed in a disc pattern in ~70% of the protoplasts (Fig. 7), whereas it was located in the small punctate staining pattern in the remaining 30% of protoplasts. AtRMR1-HA showed a disc pattern to which phaseolin colocalized in the remaining 5% of protoplasts, whereas AtRMR1-HA was in a small punctate staining pattern in 95% of transformed protoplasts (Fig. 7, e–g). Thus, 5% of transformed protoplasts had AtRMR1-HA at the PSV, which is unlike the situation when AtRMR1-HA was expressed on its own. This indicates that coexpressing phaseolin may induce the localization of AtRMR1-HA at the PSV. In addition, in 30% of coexpressing protoplasts, both phaseolin and AtRMR1-HA gave punctate staining patterns that closely overlapped (Fig. 7, i–k), which indicates that phaseolin may localize at the PVC for the PSV. These results strongly suggest that phaseolin traffics through the AtRMR1-positive compartment on its way to the PSV. Furthermore, the presence of AtRMR1-HA in the PSV when AtRMR1-HA and phaseolin were coexpressed suggests that AtRMR1-HA may traffic to the PSV together with phaseolin.

The CTPP of phaseolin is critical for its interaction with AtRMR1-HA

To further investigate the relationship between the interaction of phaseolin with AtRMR1 and the trafficking of phaseolin to the PSV, we examined whether AtRMR1-HA can interact with

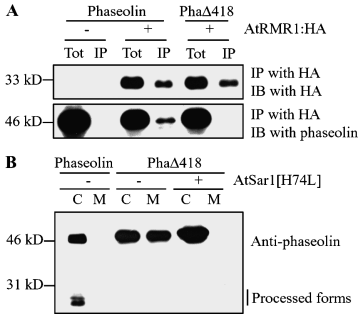

Figure 8. **The CTPP of phaseolin is critical for its interaction with AtRMR1-HA.** (A) Lack of interaction between AtRMR1-HA and phaseolinΔ418. Protein extracts (Tot) were obtained from protoplasts transformed with the indicated constructs. Immunoprecipitation (IP) was performed by using anti-HA antibody at pH 6.0 in the presence of 1 mM Ca^{2+}. The pellet fraction was then subjected to immunoblot analysis (IB) with antiphaseolin antibody. (B) COPII-dependent trafficking of phaseolin and phaseolinΔ418. Protoplasts were transformed with the indicated constructs. Protein extracts were prepared from the transformed protoplasts (C) as well as the incubation medium (M) and were analyzed by Western blotting using antiphaseolin antibody. PhaΔ418, phaseolinΔ418; side bar, the processed forms of phaseolin.

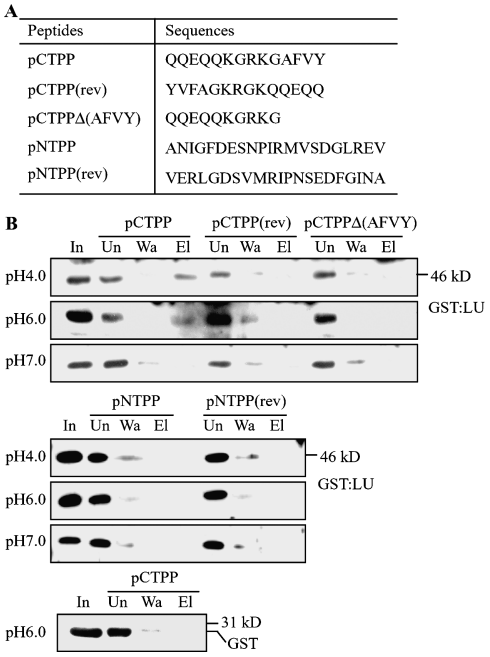

Figure 9. **The LU of AtRMR1 binds to the CTPP peptide of phaseolin.** (A) Peptide sequences. (B) In vitro binding assay. The in vitro binding assay was performed as described in Materials and methods. Peptides immobilized on Sepharose beads were incubated with purified GST-LU or GST alone under different pH conditions at 4°C. Sepharose beads were washed three times with binding buffer, and bound proteins were eluted three times with elution buffer. The unbound (Un), wash (Wa), and eluted (El) fractions were analyzed by Western blot analysis using anti-GST antibody. In, input GST-LU.

phaseolinΔ418, which lacks CTPP as a result of the deletion of four COOH-terminal amino acids. It is not targeted to the PSV but is, instead, secreted into the extracellular space (Frigerio et al., 1998; Park et al., 2004). Thus, protein extracts were prepared from protoplasts that were cotransformed with *phaseolinΔ418* and *AtRMR1-HA*, and AtRMR1-HA was immunoprecipitated by using anti-HA antibody. PhaseolinΔ418 was not detected from these immunoprecipitates (Fig. 8 A). Thus, AtRMR1-HA does not interact with phaseolinΔ418.

To exclude the possibility that the lack of interaction between AtRMR1-HA and phaseolinΔ418 is caused by the secretion of phaseolinΔ418 through some unusual pathway, we examined whether phaseolinΔ418 is secreted through the Golgi complex. Trafficking of phaseolinΔ418 was monitored in the presence and absence of AtSar1[H74L], which is a dominant negative mutant of AtSar1 that has been shown to inhibit anterograde trafficking from the ER to the Golgi complex (Takeuchi et al., 2000). We found that AtSar1[H74L] inhibits the secretion of phaseolinΔ418 and, instead, causes it to accumulate in the cell (Fig. 8 B). This indicates that, as observed previously (Frigerio et al., 1998; Park et al., 2004), phaseolinΔ418 is probably transported to the Golgi complex by COPII-mediated anterograde trafficking and is then sorted at the Golgi complex (possibly at the TGN) for secretion into the extracellular space.

The LU of AtRMR1 interacts with the COOH-terminal 14 amino acid residues of phaseolin in vitro

To further examine the interaction between AtRMR1 and phaseolin, we synthesized the peptide pCTPP, which consists of 14 amino acid residues from the phaseolin COOH-terminal region (Fig. 9 A). Two control peptides, pCTPP(rev) and pCTPPΔ(AFVY), were synthesized; pCTPP(rev) had identical amino acid residues but had a reverse sequence to that of pCTPP, and pCTPPΔ(AFVY) had a four–amino acid (AFVY) deletion in its COOH terminus. Two additional peptides, pNTPP and pNTPP(rev), were also synthesized. pNTPP consisted of 21 amino acid residues that included the NH_2-terminal sorting signal of AALP, and pNTPP(rev) had identical amino acid residues but had a reverse sequence to that of pNTPP. The LU of AtRMR1 was expressed as a GST fusion protein (GST-LU) in *Escherichia coli* and was used in the binding assay. GST-LU bound to pCTPP at pH 4.0 and 6.0 but not at pH 7.0 (Fig. 9 B, lane El). However, GST-LU did not bind to any of the other peptides — pCTPP(rev), pCTPPΔ(AFVY), pNTPP, or pNTPP(rev) — at any pH. GST alone did not bind to any of these peptides. These results strongly suggest that the LU of AtRMR1 binds specifically to the CTPP of phaseolin.

Discussion

In this study, we focused on the localization and biological function of AtRMR1 in leaf protoplasts because we found that AtRMR1 was expressed at high levels in most of the tissues that we examined regardless of the growth stage of the plant. In leaf protoplasts, both endogenous AtRMR1 and transiently expressed AtRMR1-HA give a punctate staining pattern. The majority (~77%) of both endogenous and transiently expressed AtRMR1 colocalized with ectopically expressed DIP-myc in leaf protoplasts. In addition, a minor portion (~23%) of AtRMR1-HA punctate stains colocalized with ST-GFP at the Golgi complex. However, the small punctate staining pattern of AtRMR1 was different from the disc pattern of phaseolin at the

PSV in leaf cells. Only one or two PSVs were observed in leaf cells of *A. thaliana* in contrast to the large number of PSVs in seed cells (Figs. 5 and 7; Park et al., 2004). Thus, localization of the small punctate stains that are produced by AtRMR1 and DIP-myc in leaf protoplasts is likely external to the PSV and may be the same as that observed in immature tobacco seed cells but may be different from that in root tip and mature seed cells (Jiang et al., 2000). However, the coexpression of phaseolin caused AtRMR1-HA to localize to the PSV in 5% of leaf transformed protoplasts (Fig. 7). Furthermore, the localization of AtRMR1-HA to the DIP-myc organelle was dependent on both its lumenal and cytoplasmic domains because the deletion of either domain resulted in its localization to the Golgi complex.

The exact location of the DIP-positive organelle is rather complex. DIP-positive organelles were shown to be external to the PSV in immature seed cells, whereas they were located within the PSV in mature seed and root tip cells (Jiang et al., 2000). Thus, Jiang et al. (2000) proposed that the DIP-positive organelle, which may serve as a PVC for the PSV (denoted here as PVC_P), fuses to the PSV to deliver internal proteins to the PSV. When protoplasts were cotransformed with *AtRMR1-HA* and *phaseolin*, phaseolin at the punctate stains, which were found in 30% of transformed protoplasts, colocalized with the punctate stains of AtRMR1-HA but not with those of ST-GFP. This suggests that phaseolin may be transported to the PSV through the DIP/AtRMR1-positive organelle. This notion is consistent with the idea that the DIP-positive organelle is the PVC_P (Jiang et al., 2000). In contrast, AtRMR1-HA that was expressed transiently in protoplasts did not colocalize with endogenous AtPEP12p, which is the marker protein of the PVC for the lytic vacuole (denoted here as PVC_L; da Silva Conceicao et al., 1997). This indicates that the DIP/AtRMR1-positive organelle PVC_P differs from the PVC_L. Thus, if the DIP organelle functions as a PVC, it may be specific for the PSV. In addition, these results demonstrate that plant cells have two distinct PVCs: one for the PSV and one for the lytic vacuole.

The primary structure of AtRMR1 (Jiang et al., 2000) is quite similar to that of cargo receptors such as AtVSR1/AtELP1 that are involved in protein trafficking to the vacuole (Kirsch et al., 1994; Ahmed et al., 2000; Paris and Neuhaus, 2002). The structural similarity of AtRMR1 to AtVSR1, together with its localization to the PVC_P, strongly suggests that AtRMR1 may function as a cargo receptor for PSV-destined proteins. This notion is supported by the observation that AtRMR1 deletion mutants strongly inhibited the trafficking of coexpressed phaseolin to the PSV and caused phaseolin to accumulate at the Golgi complex or to be secreted into the medium. In contrast to both endogenous AtRMR1 and transiently expressed AtRMR1-HA, which mainly localize to the DIP-positive organelle, these AtRMR1 deletion mutants mainly localized at the Golgi complex. Thus, one possible explanation for the inhibition of phaseolin trafficking by AtRMR1 mutants is that Golgi-localized AtRMR1 deletion mutants may compete with endogenous proteins, such as endogenous AtRMR1 or AtRMR1-interacting proteins, that are involved in trafficking to the PSV.

Another strong piece of evidence that supports the notion that AtRMR1 may function as a cargo receptor for PSV-destined proteins is that the CTPP of phaseolin specifically interacts with the LU of AtRMR1. This was demonstrated by in vitro binding of the GST-fused LU to the pCTPP peptide and by the coimmunoprecipitation of AtRMR1 with phaseolin, but not with phaseolinΔ418, from plant extracts. These results are consistent with the idea that CTPP is the signal sequence that directs phaseolin trafficking to the PSV (Frigerio et al., 1998). In both cases, the interaction occurred at acidic pH (pH 4.0 and 6.0) but not at neutral pH (pH 7.0). The Golgi complex is known to be acidic (Taiz, 1992; Sun-Wada et al., 2003); however, the PSV is reported to have nearly neutral pH (Swanson et al., 1998). One possible scenario that may explain the acidic pH dependency of the AtRMR1–phaseolin interaction is that although AtRMR1 mainly localizes to the PVC_P, it may traffic for sorting to the Golgi complex, where it interacts with phaseolin. Phaseolin accumulates at the Golgi complex in the presence of AtRMR1 deletion mutants, which is consistent with this hypothesis. However, in the absence of these AtRMR1 deletion mutants, we did not observe phaseolin at the Golgi complex. This may be caused by low levels of phaseolin at the Golgi complex. Once AtRMR1 has complexed with phaseolin at the Golgi complex, it may then traffic to the PVC_P. This is quite analogous to what has been observed for AtVSR1, which predominantly localizes at the PVC_L (Kirsch et al., 1994; Ahmed et al., 2000) but is also thought to travel to the TGN for sorting of lytic vacuolar proteins. At the moment, we do not know what the pH of the PVC_P is and, thus, cannot rule out the possibility that AtRMR1 remains complexed with phaseolin at the PVC_P and continues to travel with phaseolin to the PSV. Once the AtRMR1–phaseolin complex arrives at the PSV, the neutral pH in the lumen of the PSV favors dissociation of the complex. AtRMR1 molecules, once released, may then return to the PVC_P. The idea that AtRMR1 may travel to the PSV is supported by the fact that when phaseolin and AtRMR1-HA were coexpressed, 5% of transformed protoplasts showed both AtRMR1 and phaseolin at the PSV, whereas AtRMR1 that is expressed on its own is only ever found in the PVC_P or Golgi complex. The first pattern strongly suggests that AtRMR1 trafficked to the PSV together with the large amount of phaseolin and had not yet returned to the PCV_P.

In plant cells, proteins that are destined to go to the lytic vacuole are sorted at the TGN and are transported to the PVC_L for the lytic vacuole (Vitale and Raikhel, 1999; Bassham and Raikhel, 2000). In contrast, cargo proteins that are destined to go to the PSV have been proposed to be sorted at the cis half of Golgi stalk in developing DVs, and mature DVs are released from the TGN to deliver storage proteins to the PSV (Hillmer et al., 2001). However, it is not clear how these proteins are sorted at the Golgi complex. PAC vesicles that are derived from the ER have been shown to accept proteins from the Golgi complex (Hara-Nishimura et al., 1998) and, therefore, appear to function as PVC_P. However, it is not clear whether the PAC vesicle is the same as the DIP-positive organelle. Normally, PAC vesicles operate in pumpkin seed cells and are known to carry a large amount of storage proteins to the PSV directly from the ER (Hara-Nishimura et al., 1998). In this study, we have demonstrated that the PVC_P is present in proto-

plasts that are derived from leaf tissues and may function as the PVC for proteins that are delivered to the PSV through the Golgi complex. Further studies are necessary to clearly define the role of PVC_P in leaf cells.

Materials and methods

Plant material

A. thaliana (Col-O) was grown on B5 media in a growth chamber at 23°C under a light condition of 16:8 h of light/darkness. For protoplast isolation, leaf tissue was harvested 2–3 wk after germination and was immediately used.

Construction of reporter proteins

AtRMR1-HA was generated from the *AtRMR1* cDNA clone (GenBank/EMBL/DDBJ accession no. AF218807; Jiang et al., 2000) by PCR using primers RMR1-5 and RMR1-3 (all of the primer sequences are described in Table S1, available at http://www.jcb.org/cgi/content/full/jcb.200504112/DC1). The PCR products were then reamplified by using primers RMR1-5-2 and RMR1-3-2. AtRMR3 (GenBank/EMBL/DDBJ accession no. NM_102114) was amplified from genomic DNA by PCR using RMR3-5 and RMR3-3 primers. AtRMR4 (GenBank/EMBL/DDBJ accession no. NM_117024) was amplified by PCR using primers RMR4-5 and RMR4-3. The HA tag at the COOH termini of AtRMR3 and AtRMR4 was added by PCR; the primers that were used are RMR3–HA-5 and RMR3–HA-3 for AtRMR3 and RMR4–HA-5 and RMR4–HA-3 for AtRMR4. *DIP* (GenBank/EMBL/DDBJ accession no. X54855) was isolated from tobacco genomic DNA by using primers DIP-5 and DIP-3 followed by sequential PCR for myc tagging that used primers DIP-5 and DIP-3HA. To generate AtRMR1ΔLU-HA, the upstream and downstream fragments were first amplified from AtRMR1-HA by using primers RMR1-5 and ΔLU-u3 and primers ΔLU-d5 and nos-t, respectively. Subsequently, the two fragments were joined by a second PCR using ΔLU-u5 and nos-t primers. To generate AtRMR1ΔCT-HA, the upstream and downstream fragments were generated from AtRMR1-HA by primers RMR5-1 and ΔCT-u3 and primers ΔCT-d5 and nos-t, respectively. The two fragments were again joined by a second PCR using primers RMR1-5 and nos-t. The PCR products were placed under the cauliflower mosaic virus 35S promoter and nos terminator. The sequences of all of the PCR products and deletion mutants were verified by nucleotide sequencing.

Transient expression, immunofluorescent stainings, and microscopy

Plasmids were introduced by polyethylene glycol–mediated transformation (Jin et al., 2001) into protoplasts that were prepared from leaf tissues of *A. thaliana*. The expression of constructs was monitored at various time points after transformation. Images of GFP in intact protoplasts were obtained from protoplasts in incubation medium on a glass slide covered with a coverslip. For immunostaining, protoplasts on coverslips were fixed with 4% [vol/vol] PFA as previously described (Frigerio et al., 1998; Park et al., 2004). The fixed protoplasts were labeled with antiphaseolin (Frigerio et al., 1998), anti-HA (3F10; Roche Diagnostics), anti-AtPEP12p (Rose Biotechnology, Inc.), anti-myc (Santa Cruz Biotechnology, Inc.), anti–γ-COP (D.G. Robinson, University of Heidelberg, Heidelberg, Germany), anti-AtRMR1, or anti-RMR2 (J.C. Rogers, Washington State University, Pullman, WA) antibodies. Cells were washed with Tris-buffered saline washing buffer (10 mM Tris, pH 7.4, 0.9% [wt/vol] NaCl, 0.25% [vol/vol] gelatin, 0.02% [wt/vol] SDS, and 0.1% [vol/vol] Triton X-100; Park et al., 2004), and respective secondary stainings were performed for 1 h using FITC- or TRITC-labeled goat anti–rabbit or anti–rat antibodies (Molecular Probes). Immunostained protoplasts were mounted in medium (120 mM Tris, pH 8.4, and 30% glycerol) containing Mowiol4-88 (Calbiochem). Images were taken under a fluorescent microscope (Axioplan 2; Carl Zeiss MicroImaging, Inc.) equipped with a 40× plan Neofluar 0.75 objective and a cooled CCD camera (Senicam; PCO Imaging) at 20°C. The filter sets that were used are XF116 (exciter, 474AF20; dichroic, 500DRLP; and emitter, 510AF23) and XF117 (exciter, 540AF30; dichroic, 570DRLP; and emitter, 585ALP; Omega Optical). Photoshop 7.0 was used to process the images.

Protein extraction, chemical treatment, endoH digestion, and Western blot analysis

Protein extract preparations from protoplasts or incubation medium of protoplasts and EndoH digestion of AtRMR1-HA were performed as described previously (Park et al., 2004). In brief, samples were incubated with 1 mU endoH (Roche Diagnotics) at 37°C for 1 h. The reaction was then stopped by adding 5× SDS-PAGE loading buffer and was analyzed by immunoblot assays. Western blot analysis was performed by using appropriate primary and secondary antibodies as described previously (Jin et al., 2001). The protein blot was developed with an ECL detection kit (GE Healthcare), and images were obtained using an image capture system (model LAS3000; Fujifilm) or by autoradiography using an X-ray film. For Western detection of endogenous AtRMR1 and AtRMR2, protein extracts were boiled in 1× SDS-PAGE loading buffer (60 mM Tris, pH 6.8, 25% glycerol, 2% SDS, 14.4 mM β-mercaptoethanol, and 0.1% bromophenol blue) supplemented with 1 M DTT and 50 mM EDTA.

Preparation of anti-RMR1 antibody

To prepare antibody against AtRMR1, the COOH-terminal region of AtRMR1 was PCR amplified using the specific primers 5′-GAATTCATGAGACACTGGACCCAATGG-3′ and 5′-TCAACGGCTTTGACTGGATTG-3′. The PCR product was digested with EcoRI and ligated to pGEX-5X-1 (GE Healthcare) digested with EcoRI. The same COOH-terminal region was ligated in-frame to pMAL-c2 (New England Biolabs, Inc.) digested with EcoRI to produce the fusion protein, maltose-binding protein (MBP)–AtRMR1(CT). The resulting constructs, GST-AtRMR1(CT) and MBP-AtRMR1(CT), were introduced into the *E. coli* strain BL21(DE3)LysS, and the expression of these fusion proteins was induced by IPTG. GST-AtRMR1(CT) and MBP-AtRMR1(CT) fusion proteins were purified using glutathione beads (Glutathione Agarose 4B; Peptron) and amylose resin, respectively. Antibody against purified GST-AtRMR1(CT) was raised in Guinea pigs (Eurogentec) and purified using MBP-AtRMR1(CT).

Immunoprecipitation

Protein extracts were prepared in homogenization buffer (1 mM $MgCl_2$, 250 mM sucrose, and 1 mM DTT) as described in Park et al. (2004) except that the pH of the extraction buffer was adjusted to 4.0, 6.0, or 7.0 by using 20 mM of succinate, MES, and Tris-HCl, respectively. Protein extracts (100 μg of total protein) in immunoprecipitation buffer (150 mM NaCl, 1% [vol/vol] Triton X-100, and 1 mM $CaCl_2$ or 10 mM EDTA at different pH conditions) supplemented with EDTA-free protease inhibitor cocktail were incubated with protein A–Sepharose beads (CL-4B; GE Healthcare) for 30 min and centrifuged at 10,000 *g* for 5 min at 4°C. Subsequently, 4 μg anti-HA antibody (12CA5; Roche Diagnostics) was added to the supernatant and incubated for 3 h at 4°C. The immunocomplexes were precipitated with protein A–agarose for 1 h at 4°C. The pellet was then washed with immunoprecipitation buffer three times, suspended in the homogenization buffer, and analyzed by immunoblot assays.

In vitro binding assay of the LU of AtRMR1 with peptides

Five peptides (Fig. 9 A) were chemically synthesized (Anygen Inc.) and immobilized on Sepharose beads (AffiGel 10) in 10 mM citrate, pH 11.0, for pCTPP, pCTPP(rev), and pCTPPΔ(AFVY) and 10 mM MES, pH 6.0, for pNTPP and pNTPP(rev) according to the manufacturer's instructions (Bio-Rad Laboratories). To construct GST-LU, the LU (aa 1–149) of AtRMR1 was inserted in-frame into the downstream region of the GST-coding region in the pGEX vector. GST-LU fusion protein was expressed in *E. coli* and was purified by using glutathione beads according to the manufacturer's instructions. Sepharose beads that had been cross-linked to peptides were equilibrated with binding buffer (100 mM NaCl, 1% Triton X-100, and 1.0 mM $CaCl_2$) supplemented with 25 mM succinate, pH 4.0, MES, pH 6.0, or Tris-HCl, pH 7.0. Purified GST-LU was incubated with peptides that were cross-linked to Sepharose beads at 4°C overnight. After incubation, Sepharose beads were centrifuged at 5,000 rpm for 5 min at 4°C, and the supernatant was kept as the unbound fraction. Sepharose beads were then washed three times with binding buffer, and the fractions were combined (wash fraction). Finally, bound GST-LU proteins were eluted by washing the beads three times with elution buffer (25 mM Tris-HCl, pH 7.4, 150 mM NaCl, and 2% SDS), and the fractions were combined (eluted fraction). Purified GST alone was used as a control. All of the fractions were subjected to SDS-PAGE and were subsequently subjected to immunoblot analysis using anti-GST antibody (Oncogene Research Products).

Online supplemental material

Online supplemental material describes the spatial and temporal expression patterns of AtRMR1 in *A. thaliana* and the characterization of anti-AtRMR1 antibody. Fig. S1 shows the sequence alignment of AtRMR homologues. Fig. S2 shows tissue-specific and temporal expression patterns of *AtRMR1* in *A. thaliana*. Fig. S3 shows Western blot analysis of endogenous and transiently expressed AtRMR1-HA. Fig. S4 shows transient expression of epitope-tagged DIP in *A. thaliana* protoplasts. Fig. S5 shows quantification of the overlap of AtRMR1-HA with ST-GFP, γ-COP, or DIP-myc. Fig. S6 shows a schematic depiction of the constructs that were used.

Table S1 shows the primers that were used in this study. Online supplemental material is available at http://www.jcb.org/cgi/content/full/jcb.200504112/DC1.

We thank Dr. J.C. Rogers for providing the RMR clone (JR700), anti-AtRMR2 antibody, and the protocol for Western detection of AtRMR proteins. We also thank Dr. David G. Robinson for the anti–γ-COP antibody.

This work was supported by a grant from the Creative Research Initiatives program of the Ministry of Science and Technology (Korea).

Submitted: 20 April 2005
Accepted: 20 July 2005

References

Ahmed, S.U., E. Rojo, V. Kovaleva, S. Venkataraman, J.E. Dombrowski, K. Matsuoka, and N.V. Raikhel. 2000. The plant vacuolar sorting receptor AtELP is involved in transport of NH(2)-terminal propeptide-containing vacuolar proteins in *Arabidopsis thaliana*. *J. Cell Biol.* 149:1335–1344.

Bassham, D.C., and N.V. Raikhel. 2000. Unique features of the plant vacuolar sorting machinery. *Curr. Opin. Cell Biol.* 12:491–495.

Bednarek, S.Y., and N.V. Raikhel. 1991. The barley lectin carboxyl-terminal propeptide is a vacuolar protein sorting determinant in plants. *Plant Cell.* 3:1195–1206.

Cao, X., S.W. Rogers, J. Butler, L. Beevers, and J.C. Rogers. 2000. Structural requirements for ligand binding by a probable plant vacuolar sorting receptor. *Plant Cell.* 12:493–506.

Chrispeels, M.J. 1983. The Golgi apparatus mediates the transport of phytohaemagglutinin to the protein bodies in bean cotyledons. *Planta.* 158: 140–151.

Chrispeels, M.J., and N.V. Raikhel. 1992. Short peptide domains target proteins to plant vacuoles. *Cell.* 68:613–616.

da Silva Conceicao, A., D. Marty-Mazars, D.C. Bassham, A.A. Sanderfoot, F. Marty, and N.V. Raikhel. 1997. The syntaxin homolog AtPEP12p resides on a late post-Golgi compartment in plants. *Plant Cell.* 9:571–582.

Frigerio, L., M. de Virgilio, A. Prada, F. Faoro, and A. Vitale. 1998. Sorting of phaseolin to the vacuole is saturable and requires a short C-terminal peptide. *Plant Cell.* 10:1031–1042.

Frigerio, L., A. Pastres, A. Prada, and A. Vitale. 2001. Influence of KDEL on the fate of trimeric or assembly-defective phaseolin: selective use of an alternative route to vacuoles. *Plant Cell.* 13:1109–1126.

Galili, G., Y. Altschuler, and H. Levanony. 1993. Assembly and transport of seed storage proteins. *Trends Cell Biol.* 3:437–442.

Greenwood, J.S., and M.J. Chrispeels. 1985. Immunocytochemical localization of phaseolin and phytohaemagglutinin in the endoplasmic reticulum and Golgi complex of developing bean cotyledons. *Planta.* 164:295–302.

Gomez, L., and M.J. Chrispeels. 1993. Tonoplast and soluble vacuolar proteins are targeted by different mechanisms. *Plant Cell.* 5:1113–1124.

Hara-Nishimura, I., T. Shimada, K. Hatano, Y. Takeuchi, and M. Nishimura. 1998. Transport of storage proteins to protein storage vacuoles is mediated by large precursor-accumulating vesicles. *Plant Cell.* 10:825–836.

Herman, E.M., and L.M. Shannon. 1984. The role of the Golgi apparatus in the deposition of the seed lectin of *Bauhinia purpurea* (*Leguminoseae*). *Protoplasma.* 121:163–170.

Hillmer, S., A. Movafeghi, D.G. Robinson, and G. Hinz. 2001. Vacuolar storage proteins are sorted in the cis-cisternae of the pea cotyledon Golgi apparatus. *J. Cell Biol.* 152:41–50.

Hinz, G., S. Hillmer, M. Baumer, and I. Hohl. 1999. Vacuolar storage proteins and the putative vacuolar sorting receptor BP-80 exit the Golgi apparatus of developing pea cotyledons in different transport vesicles. *Plant Cell.* 11:1509–1524.

Hohl, I., D.G. Robinson, M.J. Chrispeels, and G. Hinz. 1996. Transport of storage proteins to the vacuole is mediated by vesicles without a clathrin coat. *J. Cell Sci.* 109:2539–2550.

Holkeri, H., and A. Vitale. 2001. Vacuolar sorting determinants within a plant storage protein trimer act cumulatively. *Traffic.* 2:737–741.

Jiang, L., and J.C. Rogers. 1998. Integral membrane protein sorting to vacuoles in plant cells: evidence for two pathways. *J. Cell Biol.* 143:1183–1199.

Jiang, L., T.E. Phillips, S.W. Rogers, and J.C. Rogers. 2000. Biogenesis of the protein storage vacuole crystalloid. *J. Cell Biol.* 150:755–770.

Jin, J.B., Y.A. Kim, S.J. Kim, S.H. Lee, D.H. Kim, G.W. Cheong, and I. Hwang. 2001. A new dynamin-like protein, ADL6, is involved in trafficking from the trans-Golgi network to the central vacuole in *Arabidopsis*. *Plant Cell.* 13:1511–1526.

Kim, D.H., Y.J. Eu, C.M. Yoo, Y.W. Kim, K.T. Pih, J.B. Jin, S.J. Kim, H. Stenmark, and I. Hwang. 2001. Trafficking of phosphatidylinositol 3-phosphate from the *trans*-Golgi network to the lumen of the central vacuole in plant cells. *Plant Cell.* 13:287–301.

Kinney, A.J., R. Jung, and E.M. Herman. 2001. Cosuppression of the a subunits of β-conglycinin in transgenic soybean seeds induces the formation of endoplasmic reticulum-derived protein bodies. *Plant Cell.* 13:1165–1178.

Kirsch, T., N. Paris, J.M. Butler, L. Beevers, and J.C. Rogers. 1994. Purification and initial characterization of a potential plant vacuolar targeting receptor. *Proc. Natl. Acad. Sci. USA.* 91:3403–3407.

Lee, M.H., M.K. Min, Y.J. Lee, J.B. Jin, D.H. Shin, D.H. Kim, K.H. Lee, and I. Hwang. 2002. ADP-ribosylation factor 1 of *Arabidopsis* plays a critical role in intracellular trafficking and maintenance of endoplasmic reticulum morphology in *Arabidopsis*. *Plant Physiol.* 129:1507–1520.

Matsuoka, K., S. Matsumoto, T. Hattori, Y. Machida, and K. Nakamura. 1990. Vacuolar targeting and post-translational processing of the precursor to the sweet potato tuberous root storage protein in heterologous plant cells. *J. Biol. Chem.* 265:19750–19757.

Müntz, K. 1998. Deposition of storage proteins. *Plant Mol. Biol.* 38:77–99.

Neuhaus, J.M., and J.C. Rogers. 1998. Sorting of proteins to vacuoles in plant cells. *Plant Mol. Biol.* 38:127–144.

Neuhaus, J.M., L. Sticher, F. Meins Jr., and T. Boller. 1991. A short C-terminal sequence is necessary and sufficient for the targeting of chitinases to the plant vacuole. *Proc. Natl. Acad. Sci. USA.* 88:10362–10366.

Paris, N., and J.M. Neuhaus. 2002. BP-80 as a vacuolar sorting receptor. *Plant Mol. Biol.* 50:903–914.

Park, M., S.J. Kim, A. Vitale, and I. Hwang. 2004. Identification of the protein storage vacuole and protein targeting to the vacuole in leaf cells of three plant species. *Plant Physiol.* 134:625–639.

Pimpl, P., A. Movafeghi, S. Coughlan, J. Denecke, S. Hillmer, and D.G. Robinson. 2000. In situ localization and in vitro induction of plant COPI-coated vesicles. *Plant Cell.* 12:2219–2236.

Saalbach, G., M. Rosso, and U. Schumann. 1996. The vacuolar targeting signal of the 2S albumin from Brazil nut resides at the C terminus and involves the C-terminal propeptide as an essential element. *Plant Physiol.* 112:975–985.

Shimada, T., E. Watanabe, K. Tamura, Y. Hayashi, M. Nishimura, and I. Hara-Nishimura. 2002. A vacuolar sorting receptor PV72 on the membrane of vesicles that accumulate precursors of seed storage proteins (PAC vesicles). *Plant Cell Physiol.* 43:1086–1095.

Shimada, T., K. Fuji, K. Tamura, M. Kondo, M. Nishimura, and I. Hara-Nishimura. 2003. Vacuolar sorting receptor for seed storage proteins in *Arabidopsis thaliana*. *Proc. Natl. Acad. Sci. USA.* 100:16095–16100.

Sohn, E.J., E.S. Kim, M. Zhao, S.J. Kim, H. Kim, Y.W. Kim, Y.J. Lee, S. Hillmer, U. Sohn, L. Jiang, and I. Hwang. 2003. Rha1, an *Arabidopsis* Rab5 homolog, plays a critical role in the vacuolar trafficking of soluble cargo proteins. *Plant Cell.* 15:1057–1070.

Sun-Wada, G.H., Y. Wada, and M. Futai. 2003. Vacuolar H^+ pumping ATPases in luminal acidic organelles and extracellular compartments: common rotational mechanism and diverse physiological roles. *J. Bioenerg. Biomembr.* 35:347–358.

Swanson, S.J., P.C. Bethke, and R.L. Jones. 1998. Barley aleurone cells contain two types of vacuoles. Characterization Of lytic organelles by use of fluorescent probes. *Plant Cell.* 10:685–698.

Taiz, L. 1992. The plant vacuole. *J. Exp. Biol.* 172:113–122.

Takeuchi, M., T. Ueda, K. Sato, H. Abe, T. Nagata, and A. Nakano. 2000. A dominant negative mutant of sar1 GTPase inhibits protein transport from the endoplasmic reticulum to the Golgi apparatus in tobacco and *Arabidopsis* cultured cells. *Plant J.* 23:517–525.

Toyooka, K., T. Okamoto, and T. Minamikawa. 2000. Mass transport of proform of a KDEL-tailed cysteine proteinase (SH-EP) to protein storage vacuoles by endoplasmic reticulum-derived vesicle is involved in protein mobilization in germinating seeds. *J. Cell Biol.* 148:453–464.

Vitale, A., and N.V. Raikhel. 1999. What do proteins need to reach different vacuoles? *Trends Plant Sci.* 4:149–155.